

1 Exploiting stagnant conditions to derive robust emission ratio estimates for 2 CO₂, CO and Volatile Organic Compounds in Paris

3

4 L. Ammoura¹, I. Xueref-Remy¹, F. Vogel¹, V. Gros¹, A. Baudic¹, B. Bonsang¹, M. Delmotte¹, Y.
5 Té², and F. Chevallier¹

6 ¹LSCE, Unité mixte CEA-CNRS-UVSQ, UMR 8212, 91191 Gif-Sur-Yvette, France

7 ²LERMA, Unité mixte CNRS-ENS-OP-UCP-UPMC, UMR 8112, 75005 Paris, France

8

9

10 Abstract

11 We propose an approach to estimate urban emission ratios that takes advantage of the
12 enhanced local urban signal in the atmosphere at low wind speed. We apply it to estimate
13 monthly ratios between CO₂, CO and some VOCs from several atmospheric concentration
14 measurement datasets acquired in the centre of Paris between 2010 and 2014. We find that
15 this approach is little sensitive to the regional background level definition and that, in the
16 case of Paris, it samples all days (weekdays and weekends) and all hours of the day evenly. A
17 large seasonal variability of the $\Delta\text{CO} / \Delta\text{CO}_2$ ratio in Paris is shown, with a difference of
18 around 60% between the extreme values and a strong anti-correlation ($r^2=0.75$) with
19 atmospheric temperature. The comparison of the ratios obtained for two short
20 measurement campaigns conducted in two different districts and two different periods (fall
21 and winter) shows differences ranging from -120% to +63%. A comparison with a highly
22 resolved regional emission inventory suggests some spatial variations of the ratio within the
23 city.

24

25 1. Introduction

26 In response to changing air quality and climate, there is a growing interest in
27 quantifying emissions of pollutants and greenhouse gases from urban areas (UNEP 2013,
28 EEA 2014). Urban emissions are usually known through the combination of direct and
29 indirect geospatial energy use statistics with emission factors for individual source sectors.
30 The heterogeneity of the input data in space, time and type makes it difficult to monitor the
31 uncertainties of these inventories. Such monitoring actually receives little incentive at the
32 international level (e.g., Bellasseem et al. 2015), but it has been an active topic for scientific
33 research. Some studies have been based on measurement campaigns dedicated to specific
34 sectors, for instance air-composition measurements in road tunnels for traffic emissions

35 (e.g., Touaty and Bonsang, 2000 ; Ammoura et al., 2014), or in ambient air for power plants
36 (Zhang and Schreifels, 2011), waste water treatment plants (Yoshida et al., 2014 ; Yver-
37 Kwok et al. 2015) or for the overall city-scale emissions (Lopez et al., 2013; Turnbull et al.,
38 2011, 2015, Xueref-Remy et al., 2016). Measurements made in the ambient air are affected
39 by dilution in the atmospheric boundary layer, but this effect cancels out for mole fraction
40 ratios between the considered species. The mole fraction ratios estimated from ambient air
41 can also be directly interpreted in terms of emission ratios provided that the measured
42 molecules share the same origin (e.g., Turnbull et al., 2006). Ultimately emission ratios may
43 be interpreted in terms of sectoral emissions. In practice, the mixing of air parcels of various
44 origins and ages largely hampers the interpretation. To isolate the local urban signal,
45 measurements for species with a significant life time in the atmosphere have to be corrected
46 from background influence (Turnbull et al., 2015), usually based on other measurements
47 made in the free troposphere or at a remote site (e.g., Lopez et al. 2013; Turnbull et al.,
48 2015). Isotopic measurements, like those of $^{14}\text{CO}_2$, can also allow the analysis to be more
49 specifically focused on anthropogenic activities (e.g., Levin and Karstens, 2007; Turnbull et
50 al., 2011). Last, atmospheric transport models are used in a few studies to quantify the
51 contributions of the different sources within an inverse modelling approach (e.g., Saide et al.
52 2011, Lauvaux et al., 2013; Bréon et al. 2015).

53 Here, we investigate the possibility of benefiting from an enhanced local urban signal
54 at low wind speed for estimating emission ratios from atmospheric composition
55 measurements. Indeed, when the atmosphere is not well ventilated, emission plumes get
56 trapped in the atmospheric boundary layer close to their origin. The resulting large peaks in
57 mole fractions time-series are easily visible compared to typical background variations. In
58 this manuscript, we make the first attempt to fully exploit this well understood behaviour.
59 We use several measurement campaigns of CO_2 , CO and Volatile Organic Compounds (VOCs)
60 performed in Paris in 2010, 2013 and 2014 to validate the approach and to evaluate local
61 emissions ratios. Paris is the third largest megacity in Europe and the largest one in France.
62 It comprises around 12 million people when including its suburbs. The population density is
63 one of the highest in Europe with 21347 inhabitants per km^2 (INSEE, 2014). According to the
64 latest Paris inventory of Airparif (Association in charge of monitoring the air quality in the
65 Paris region) provided for year 2010, emissions of CO_2 are mainly from the traffic (29%) and
66 residential and service sectors (43%) (Airparif, 2013). Airparif also estimated VOC emissions
67 and their main anthropogenic origins are the same as those of CO_2 (such as traffic or
68 residential heating).

69 The paper is structured as follows. Section 2 presents the measurements and the
70 data. Section 3 starts with a presentation of typical measurements and a discussion about
71 the choice of the background level, presenting two different options. The analysis method
72 itself developed to estimate urban emission ratios is described in Section 3.3 including
73 sensitivity tests (Sections 3.3.2 and 3.3.3). Section 4 presents the results obtained for
74 different periods of the year and different years. Section 4.1 gives the interpretation of the

75 ratios determined with our method and discusses the representativeness of these ratios.
76 Section 4.2 presents the seasonal variability of the $\Delta\text{CO}/\Delta\text{CO}_2$ ratio in Paris and Section 4.3
77 compares all ratios between co-emitted species obtained during two short campaigns in
78 Paris.

79 **2. Methods**

80 **2.1 Site description**

81 All atmospheric composition measurements presented in this study have been made
82 in the centre of Paris. The instruments were installed at two sites. The first one is located on
83 the Jussieu campus of University Pierre et Marie Curie (UPMC) at the QualAir station
84 (<http://qualair.aero.jussieu.fr>). This station stands on the roof of a building, on the left bank
85 of the river Seine (48°50'N, 2°21'E and 23 m above ground level). A botanical garden of 28
86 hectares, the Jardin des Plantes, lies about 500 m from the measurement site. The closest
87 motorways are about 4 km on the south and on the south-east, but the university is
88 surrounded by many streets which are particularly congested during rush hours. The
89 emission activities in the centre of Paris essentially originate from road traffic activities and
90 from the residential and service sectors, since most industrial activities have been removed
91 in the 1960s (AIRPARIF, 2013).

92 The second measurement site is the roof of Laboratoire d'Hygiène de la Ville de Paris
93 (LHVP) located about 2 km from the Jussieu campus, south-east of it (48°49'N and 2°21'E
94 and 15 m above ground level). It dominates a public garden of 4.3 hectares, the Parc de
95 Choisy. Residential buildings and arterial roads also surround this site. The closest
96 expressway is a few hundred meters south of the site.

97

98 **2.2 Instrumentation and air sampling**

99 **2.2.1 Joined MEGAPOLI/CO₂-Megaparis winter campaign**

100 Our first campaign was performed jointly within the MEGAPOLI European project
101 (Megacities: Emissions, urban, regional and Global Atmospheric POLLution and climate
102 effects, and Integrated tools for assessment and mitigation project, <http://megapoli.info/>)
103 and the CO₂-Megaparis project (<https://co2-megaparis.lsce.ipsl.fr>). This 'winter campaign'
104 took place in Paris during January-February 2010 (Dolgorouky et al. 2012, Lopez et al. 2013).

105 Two instruments were deployed at the LHVP. A Gas Chromatograph equipped with a
106 Flame Ionisation Detector (GC-FID, Chromatotec) sampled Non-Methane Hydrocarbons
107 (NMHCs). Mole fractions of acetylene, ethylene, propene, *i*-pentane, *n*-pentane, ethane and
108 propane were obtained with a time resolution of 30 minutes (air is sampled during the first
109 10 minutes and analysed during the next 20 minutes). More details can be found in Gros et
110 al. (2011) and Dolgorouky et al. (2012).

111 A Cavity Ring-Down Spectrometer (CRDS G1302, Picarro Inc) was also deployed to
112 analyse CO₂, CO and H₂O mole fractions with a time resolution of 1 s (see Lopez et al., 2013,
113 for more details).

114

115 **2.2.2 Long-term continuous CO₂ and CO measurements**

116 A Cavity ring-Down analyser (CRDS G1302, Picarro Inc.) performed continuous CO₂,
117 CO and H₂O measurements in Jussieu from 4 February 2013 to 11 June 2014 with a time
118 resolution of 1 s. This instrument was calibrated about every two months using three 40 L
119 aluminium gas tanks. These cylinders were previously calibrated for CO₂ and CO dry air mole
120 fractions against the NOAA-X2007 scale for CO₂ and the NOAA-X2004 for CO. A fourth gas
121 cylinder was used as a target to evaluate the repeatability of the data and the drift of the
122 instrument. This target was analysed for 20 minutes every 12 h between 4 February 2013
123 and 25 August 2013 and for 15 minutes every 47 h since 26 August 2013. Using the target
124 gas measurements, we estimate the repeatability and the trueness (closeness of agreement
125 between the average of a huge number of replicated measured species concentrations and a
126 reference concentration, BIPM (2012)) of the 1 minute averaged data to be, respectively,
127 0.05 ppm and 0.03 ppm for CO₂ and 6.8 ppb and 3.7 ppb for CO. The instrument was
128 compared to the MEGAPOLI/CO₂-Megaparis one used in 2010 and the repeatability and the
129 trueness of the 1 min averages data were found to be almost the same.

130

131 **2.2.3 'Multi-CO₂' field-campaign**

132 Several instruments were installed next to the CRDS analyser in Jussieu from 11
133 October 2013 until 22 November 2013 within the Multi-CO₂ project.

134 For the compounds of interest for this study (CO₂, CO and light VOCs), the same
135 instruments that were used during the joined MEGAPOLI/CO₂-Megaparis campaign were
136 deployed (see Section 2.2.1). VOC mole fractions were measured using a gas chromatograph
137 (Chromatotec) calibrated against a reference standard (National Physics Laboratory,
138 Teddington, UK). Some VOCs were selected for this study because they share the same
139 origins (such as traffic or residential heating) than other VOCs, CO and CO₂: ethane,
140 ethylene, acetylene, propane, propene, i-pentane and n-pentane. The total uncertainty of
141 the data was estimated to be better than 15%.

142 Meteorological parameters (wind speed and direction, temperature) were also
143 monitored (instrument WMR2000, OREGON Scientific).

144

145

146

147 **2.3 Data processing**

148 As the time resolution was different for both instruments (CRDS and GC-FID), the
149 data have been synchronized. The chosen time interval was the one imposed by GC-FID
150 measurements. Data from GC-FID were acquired for 10 minutes every 30 minutes, the given
151 time stamp corresponding to the beginning of the measurement. Thus for each compound
152 measured by the other instruments (CRDS and meteorological instruments), data have been
153 averaged on the same 10 minutes interval. Finally, in this study, all the data have a same
154 time step of 30 minutes.

155

156 **3. Results**

157 **3.1 Typical time series and identification of specific meteorological events**

158 Figure 1 shows an example of atmospheric gas dry air mole fractions time series
159 collected during the Multi-CO₂ campaign in 2013, with a time step of 30 min. The wind speed
160 during the same period is also represented on the figure (1e). Time series recorded during
161 the joined MEGAPOLI/CO₂-Megaparis campaign in 2010, as well as the continuous
162 measurements of CO₂ and CO in Jussieu are shown in the supplementary material.

163 Mole fractions of the different species appear to co-vary much, despite the different
164 lifetime of the species: CO₂ and CO have typical life time in the atmosphere (τ) much longer
165 than the observation period whereas acetylene has a τ of a 13 days and ethylene has a τ of a
166 few hours. In comparison, the meteorological events in Paris during the campaign lasted
167 from a few hours to one day so that VOCs with a τ longer than two days, like acetylene, can
168 be almost considered as non-reactive species. For shorter-lived species, here only ethylene
169 and propene (1 day $>$ τ $>$ 5 hours), we computed the correlations between these species and
170 acetylene. When considering all the data of the Multi-CO₂ campaign (without any selection),
171 coefficients of determination are high ($r^2 > 0.70$). These tight correlations between VOCs with
172 different reactivity suggest a limited impact of the chemistry.

173 In Figure 1, we identify some events when the mole fractions of all species were
174 significantly higher than elsewhere over the campaign duration (1.25 to 6 times as high).
175 These periods (30 and 31 October, 10 and 11 November) appear to be systematically linked
176 to specific meteorological conditions when the wind speed was very low (less than 1 m.s⁻¹).
177 The mole fractions obviously increased as the result of the stagnation of local emissions in
178 the atmosphere. However, three periods with low wind speed do not correspond to
179 significant peaks in mole fractions (on 5, 6 and 7 November 2013). These 3 periods were too
180 short (they last around 2h) for the accumulation of emissions in the atmosphere to have
181 taken place and did not result in high mole fractions. There is one more period that we can

182 highlight and for which the wind speed was less than $1 \text{ m}\cdot\text{s}^{-1}$, from 17 November 15:00 (UTC)
183 to 18 November 7:00 (UTC). The mole fractions were higher than the common baseline due
184 to changes in synoptic conditions. However, no significant peaks are visible. We notice that
185 during this period, even though the wind speed was low, wind came from one sector only
186 (from 90 to 190°) whereas there is no specific wind direction associated to the large peaks of
187 the other periods (turning wind, see Figure 2 (a)). In the case of a dominant wind direction,
188 and despite low wind speeds, emissions did not seem to have accumulated in the
189 atmosphere (there may have been slowly evacuated). The wind roses in the two different
190 cases are represented in Figure 2. To summarise, periods with low wind speed and non-
191 directional winds are the focus of the present study because they show a distinct local
192 emission signal in the mole fractions.

193

194 **3.2 Background levels**

195 The previous data selection does not remove all influence of long-range transport
196 (advection) and dispersion in the measurements and there is still a need to remove a
197 background level, especially in the case of species with significant lifetime in the atmosphere
198 like CO_2 . Most of the previous studies whose main interest was CO_2 defined a continental
199 clear-air background to correct the CO_2 data. For example, data from Mace Head in Ireland
200 (Lopez et al., 2013) or from Jungfraujoch in Switzerland (Vogel et al., 2010) are often
201 considered as background data for measurements in Europe, but strictly speaking they are
202 too far from Paris to isolate the city signal. Measurements in the free troposphere have also
203 been used as a baseline (Miller et al., 2012; Turnbull et al., 2011), but are particularly
204 expensive to make and are not available for our study period. Furthermore, continental and
205 free-tropospheric measurements may be misleading for the interpretation of local emissions
206 (Turnbull et al., 2015). For short-lived species, the definition of the background is not as
207 critical and the smallest measured value is often used.

208 Here, we investigate two options to define the urban background levels. The first
209 option takes advantage of the fact that the urban emissions are positive fluxes, i.e. which
210 increase local atmospheric mole fractions. We define background mole fractions as all
211 measurements smaller than the fifth percentile of the species over a moving window. The
212 moving window allows accounting for the dependence of the background on the synoptic
213 situation or on the time of year, as the background changes seasonally for many gases. As
214 the average characteristic time of synoptic changes is a few days, and in order to gather a
215 significant amount of data, we define overlapping windows of three days that start every day
216 at 00:00 (UTC), in increments of 1 day. Figure 1 displays the selected lowest 5% as black disks
217 for some species measured during the Multi- CO_2 campaign. In order to avoid discontinuities,
218 we linearly interpolate the selected data to obtain a background mole fraction time series
219 with a time resolution of 30 minutes (black curves on Figure 1).

220 This background definition is simple to implement because it does not require
221 additional measurements. It samples different wind sectors and not just clean air ones. For
222 instance, we noticed a difference of 8 ppm between continental (0-180°) and oceanic (180-
223 360°) sectors for the averaged CO₂ background derived from the 5th percentile calculation.
224 This background definition is expected to work well for all species that do not have local
225 sinks in the atmosphere or at the surface. We saw in Section 3.1 that chemical sinks can be
226 neglected for our measurements, but in the case of CO₂ during the vegetation-uptake season
227 (summer in particular), vegetation within Paris also contributes to populating the fifth
228 percentile.

229 Our second option (for CO₂ only) defines the background from a publicly available
230 analysis of the global atmospheric composition. We test it for CO₂, the species for which the
231 first definition may be the least appropriate. The definition of the background level of CO₂
232 relies on the global inversion product of the Monitoring Atmospheric Composition and
233 Climate project (MACC v13.1, <http://www.copernicus-atmosphere.eu/>,
234 Chevallier et al., 2010). This product has a resolution of 3.75° × 1.9° (longitude-latitude) in space and of 3 h in
235 time. It combines the information from 131 CO₂ stations over the globe and a transport
236 model within a Bayesian framework and estimates the CO₂ surface fluxes over the globe
237 together with the full 4D CO₂ field.

238 We extracted the 3-hourly time series of the CO₂ concentrations from the MACC
239 database for the eight grid points that surround our two measurement sites, Jussieu and the
240 LHVP. The CO₂ background mole fraction is estimated as the linear interpolation in time of
241 the analysed CO₂ concentrations averaged over the eight grid points. In the following, we call
242 $\Delta species$, the mole fractions excess from the background as defined by either method.

243 A comparison of the results obtained using the two background definitions
244 successively is presented in Section 3.3.3.

245

246 **3.3 Determination of the ratios between co-emitted species**

247 **3.3.1 Description of the method**

248 We present next the method to evaluate ratios of excess mole fractions between 2
249 species ($\Delta species_1$ and $\Delta species_2$). We consider a moving window of 4 h in increments of 30
250 minutes (each period contains 8 points). On each period, we compute the coefficient of
251 determination r^2 between $\Delta species_1$ and $\Delta species_2$ and use a linear regression to evaluate
252 the slope (type II model regression in which errors on both axes are accounted for). This
253 slope defines a ratio between the two considered $\Delta species$ over the 4h period. We also
254 calculate the difference between maximum and minimum $\Delta species_1$, which is plotted on the
255 x axis, over this period (we name it $\delta \Delta species_1$). The motivation for this amplitude
256 computation will be developed in Section 4.1. These calculations are made if more than 5

257 points exist during the time period and if species excesses are linearly related (a p -value test
258 relative to linear relationship of species excesses is conducted and p -value <0.001 are
259 selected). As an example, on a 4h period, we compute (i) the coefficient of determination r^2
260 between ΔCO and ΔCO_2 , (ii) the slope, which well fits the considered dataset (thus giving the
261 $\Delta\text{CO}/\Delta\text{CO}_2$ ratio over this period) and (iii) $\delta\Delta\text{CO}_2$.

262 In Figure 3, we show some examples of ratios determined on each 4h period against
263 the local corresponding species offset $\delta\Delta\text{CO}_2$. They have a simple structure with a horizontal
264 asymptote when $\delta\Delta\text{CO}_2$ is high. The equation of the asymptote defines the average ratio.
265 Interpretation and representativeness of this ratio are discussed in Section 4.1.

266 In order to unambiguously define the equation of this horizontal asymptote, and the
267 related value of the ratio, we apply a filter on r^2 and on $\delta\Delta\text{species}_1$ that isolates the
268 asymptote. We apply this criterion to measurements spread over a month. The sensitivity of
269 the ratios to all tested criteria is presented in Section 3.3.2. The final choice of a criterion is a
270 compromise between a cautious selection of points (derived from the criterion on r^2 and
271 $\delta\Delta\text{species}_1$) to clearly extract the local-signal asymptote, and a selection of enough points to
272 get a robust ratio. Finally, the equation of the horizontal asymptote is the ratio (we impose a
273 slope of zero). The ratio uncertainty is computed at a confidence level of 68% (1- σ).

274

275 3.3.2 Sensitivity to the criterion on r^2 and $\delta\Delta\text{CO}_2$

276 We present here a sensitivity test for the criterion on r^2 and $\delta\Delta\text{CO}_2$ in the case of the
277 $\Delta\text{CO}/\Delta\text{CO}_2$ ratio during the Multi- CO_2 campaign. We evaluate this ratio using the method
278 described in Section 3.3.1 and vary the thresholds on r^2 (with values 0.6, 0.7, 0.8 and 0.9)
279 and on $\delta\Delta\text{CO}_2$ (with values 15, 20, 25, 30, 35 and 40 ppm).

280 Considering a given r^2 ($\delta\Delta\text{CO}_2$ can vary and be higher than 15, 20, 25, 30, 35 or 40
281 ppm), we find less than 10% difference between all the derived ratios. For the other case,
282 considering a fixed $\delta\Delta\text{CO}_2$ offset and a varying r^2 , differences between all ratios were found
283 to be less than 6%. However, tighter restrictions on the criterion result in fewer available
284 data points that sample the emission conditions within the month less well. As an example,
285 for the couple ($r^2>0.6$, $\delta\Delta\text{CO}_2>15\text{ppm}$), 211 points are selected in the asymptote whereas for
286 the one ($r^2>0.9$, $\delta\Delta\text{CO}_2>30\text{ppm}$), only 39 points remain. We choose the criterion $r^2>0.8$ and
287 $\delta\Delta\text{CO}_2>20\text{ppm}$ to determine the $\Delta\text{CO}/\Delta\text{CO}_2$ ratio during the Multi- CO_2 campaign: it keeps
288 more than a hundred points to define the asymptote. The same test was conducted on all
289 studied ratios and differences between derived ratios do not exceed 10%, which is lower
290 than the 15% error imposed by the uncertainty on VOC data. The data selection for several
291 ratios, including $\Delta\text{CO}/\Delta\text{CO}_2$, is presented on Figure 3.

292

293

3.3.3 Sensitivity to the background choice

294 In this section, we test the influence of the chosen background definition on the
295 obtained $\Delta\text{CO}/\Delta\text{CO}_2$ ratio using the methods described in Section 3.3.1. We compare $\Delta\text{CO}/$
296 ΔCO_2 ratios for 2013 using the 5th percentile or MACC simulations as background levels
297 (MACC simulations for 2014 were not available when this study was conducted). The
298 evolution of the ratios for both options is presented in Figure 5. We evaluate the relative
299 difference between the ratios derived from the two options (in % of the ratio obtained with
300 the fifth percentile as background). Differences vary from -17% in August 2013 to +11% in
301 September 2013. The highest differences are found for the summer months (11% on
302 average), and the lowest ones for the winter months (3.2% on average). These results show
303 that the definition of the background does not significantly affect the derived ratios, even
304 during the summer months when MACC and its 3-hourly resolution explicitly account for the
305 daily cycle of vegetation activity, while the 3-day moving window does not. This comes from
306 the fact that urban mole fractions during low wind speed periods are usually larger enough
307 than the background mole fractions (from around 1.25 to 6 times more).

308 After these analyses, we finally choose to define background levels using the fifth
309 percentile on a running window of 3 days as described in Section 3.2.1. However, tests were
310 conducted using the tenth percentile (and a running window of 3 days) or changing the
311 length of the running window between 1 and 5 days (but still considering the fifth
312 percentile). No significant difference was found using the tenth percentile (less than 2%
313 difference between the two derived $\Delta\text{CO}/\Delta\text{CO}_2$ ratios). Comparing $\Delta\text{CO}/\Delta\text{CO}_2$ ratios
314 obtained with different lengths of the running window, ratios differ by less than 6% from
315 one case to another, thus consolidating our choice for background levels.

316

317 4. Discussion

318 We apply the method presented in Section 3.3.1 to assess ratios between co-emitted
319 species in Paris. In this section, we first discuss the interpretation and the representativeness
320 of the ratios determined using the method previously presented. Then, we divide the
321 analysis in two parts. First we focus on the seasonal variability of the $\Delta\text{CO}/\Delta\text{CO}_2$ ratio using
322 continuous measurements acquired from February 2013 to June 2014. Then we compare the
323 ratios between co-emitted species and CO_2 obtained for the two short campaigns (in Section
324 4.3).

325

326

327 **4.1 Interpretation and representativeness of the ratios determined with the** 328 **asymptotic method**

329 The x axis in Fig. 3 ($\delta\Delta_{\text{species}_1}$) represents the variability of the species excess over a
330 4h-period. Large values correspond to a strong increase or decrease in the species local
331 emissions, and highlight the concentration peaks that occur at low wind speed. The presence
332 of an asymptotic value in the monthly ratio plots like that of Fig. 3 suggests that the ratios do
333 not vary much within the month. This stability is also confirmed by the regular spread of the
334 selected events throughout the month and even throughout the day. For instance, applying
335 our method to the continuous CO and CO₂ measurements acquired in 2013/2014 in Paris,
336 we notice that all days (weekdays and weekends) and all hours of the day were sampled
337 equally: no period type is systematically missing (see Figure 4). This feature allows our
338 method to yield a robust average ratio per month in Paris despite, e.g, boundary layer
339 dynamics during the day.

340 Our study focuses on low wind speed periods (less than 1 m.s⁻¹, i.e. less than 3.6
341 km.h⁻¹). Considering this speed and a typical event length of about 3h, the extension of the
342 influence zone would be a circle with a radius of 11 km if the wind direction was constant.
343 With a non-directional wind, as in our case, the influence area is much smaller, likely
344 spreading only a few hundred meters around the site. Urban model simulations could
345 confirm this point but this would involve different resources and expertise than those of our
346 study.

347

348 **4.2 Seasonal variability of the $\Delta\text{CO}/\Delta\text{CO}_2$ ratio in Paris**

349 The evolution of the $\Delta\text{CO}/\Delta\text{CO}_2$ ratios in Jussieu between March 2013 and May 2014
350 is presented in Figure 5. It shows a large seasonal variability with a maximum value in winter
351 and a minimum value in summer. There is a difference of around 60% between these
352 extreme values (minimum value: 3.01 ppb/ppm, maximum value: 6.80 ppb/ppm). The
353 impact of the biosphere in this seasonality seems to be negligible because night-time and
354 day-time measurements yield the same ratios (i.e. the same asymptotes with our method).

355 Given the large seasonal cycle observed, we hypothesise that temperature is an
356 important driver of the $\Delta\text{CO}/\Delta\text{CO}_2$ ratio. The monthly atmospheric temperature measured
357 during the low wind speed periods is also shown in Figure 5. The two curves are much anti-
358 correlated ($r^2=0.75$): when the temperature is high, the ratio is low - and reciprocally. This is
359 likely the consequence of higher emissions when temperatures are low because residential
360 heating is important whereas in summer, when temperatures are high, emissions mainly
361 come from traffic, residential cooking and service sectors which all together seem to
362 correspond to a lower $\Delta\text{CO}/\Delta\text{CO}_2$ ratio. The difference in emissions between the two

363 extreme seasons relies on the importance of residential heating use. The differences in the
364 ratios may indicate that higher ratios are observed for residential heating than for other
365 sources. This is not in agreement with data from the Airparif inventory (2010): the annual
366 CO/CO₂ for residential heating and for the other sectors are respectively 2.7 ppb/ppm and
367 7.1 ppb/ppm. However, we cannot exclude the impact of other drivers such as traffic as
368 several studies previously showed that CO emissions are more important when vehicles
369 work at lower temperature than the optimal value (Ammoura et al., 2014; SETRA, 2009).
370 However, to our best knowledge, no study characterised the link between vehicle emissions
371 and ambient temperature so far. The Airparif inventory does not show a seasonal variability
372 as there is almost no difference on CO/CO₂ ratios between winter and summer: 3.1 ppb/ppm
373 in January against 3.6 ppb/ppm in August. The comparison between these estimates and our
374 observations suggests the possible influence of another source. Indeed, wood burning is a
375 major part of CO emissions from the residential sector (around 90%) the Airparif inventory
376 does not include biogenic and/or natural sources of CO₂ for two reasons (Airparif, 2013): 1/
377 Airparif respects the definitions given by the UNFCCC; and 2/ the carbon cycle of the
378 biomass lifetime is estimated too short to account for this emission sector. However, our
379 study shows that CO₂ emissions from biomass burning might represent a non-negligible part
380 of the Paris CO₂ budget, but we could not confirm it. The differences may be adjusted
381 accounting for this source also for CO₂ emissions and may explain that there is no seasonal
382 variability in the Airparif inventory. However, we were not able to evaluate this point in our
383 study.

384

385 **4.3 Comparison between Multi-CO₂ and MEGAPOLI/CO₂-Megapolis campaigns**

386 **4.3.1 CO to CO₂ emission ratios in Paris**

387 The ratios between the co-emitted species for the Multi-CO₂ and MEGAPOLI/CO₂-
388 Megapolis campaign, derived from our method, are presented in Table 1.

389 Generally, ratios are different between the two campaigns. We notice differences
390 from -120% to +63%. A satisfactory agreement is found between the two campaigns for the
391 ratios that are reported in bold in Table 1 (less than 15% of difference). Several explanations
392 can be given for these differences. First, measurements were not carried out in the same
393 year: 2010 for the joined MEGAPOLI-CO₂-Megapolis campaign and 2013 for the Multi-CO₂
394 one. The differences in the ratios may illustrate some evolution in the emission structure (as
395 an example, some technological improvements can occur for vehicles or heating systems).
396 Secondly, these differences may highlight the importance of the seasonal variability of the
397 ratios, which was shown in Section 4.2. Indeed, measurements were performed in autumn
398 (October-November) for the Multi-CO₂ campaign and in winter (January-February) for the
399 MEGAPOLI/CO₂-Megapolis one. The $\Delta\text{CO} / \Delta\text{CO}_2$ ratio from the latter campaign is also
400 reported in Figure 5 for the corresponding month of the year: it aligns well on the seasonal

401 variability observed in Jussieu, even though this campaign was made four years before.
402 Furthermore, average temperatures during the low wind speed periods were not the same:
403 10°C during the Multi-CO₂ campaign, 3°C during the MEGAPOLI/CO₂-Megapolis one. This is
404 in agreement with the argument developed in Section 4.2: residential heating is more
405 important in the heart of winter and its emissions make the $\Delta\text{CO} / \Delta\text{CO}_2$ ratio higher. Finally
406 the instruments were not installed at the same location in the centre of Paris (there are 2 km
407 between the two locations). Thus the emission area of influence could be different because
408 the local activities are not exactly the same around the two sites. As an example,
409 expressways, where the vehicle speed is limited to 80 km.h⁻¹ and the vehicle flow is high, are
410 closer to the LHVP (MEGAPOLI/CO₂-Megapolis measurements), leading this site to be more
411 influenced by large traffic emissions. This spatial variability of the ratios in Paris is confirmed
412 by the Paris emission inventory Airparif 2010. Airparif provides annual CO and CO₂ emissions
413 by districts in Paris. Jussieu is in the 5th district and the LHVP in the 13th. According to the
414 latest Airparif inventory, the annual CO/CO₂ ratios are respectively 2.43 ppb/ppm and 3.74
415 ppb/ppm for the 5th and the 13th districts. However, the good agreement between the ratio
416 from the MEGAPOLI/CO₂-Megapolis campaign (measurements in 2010) and the one derived
417 in Jussieu (measurements in 2014) indicates that the seasonal variability is the main driver
418 for the evolution of the ratios.

419 **4.3.2 VOCs emission ratios in Paris: Multi-CO₂ vs MEGAPOLI/CO₂-Megapolis**

420 This section analyses the VOC emission ratios more specifically, as these compounds
421 (which share common sources with CO and CO₂) were also measured during the two
422 campaigns (Multi-CO₂ and MEGAPOLI/CO₂-Megapolis). In the presence of nitrogen oxides
423 (NO_x), VOC oxidation lead to the formation of ozone and secondary organic aerosols, which
424 impacts air quality and climate. Therefore characterizing VOC emissions in urban areas
425 (which are always associated to high NO_x conditions) is of importance. VOCs include a large
426 variety of compounds and information on their sources and sinks will be given here only for
427 the compounds selected in this study. As already mentioned, among the various non-
428 methane hydrocarbons measured during these campaigns, the selected compounds were
429 the ones which presented a strong correlation with CO₂ and CO ($r^2 > 0.8$), allowing the use of
430 our approach for the ratio determination. In urban areas, anthropogenic sources of VOCs are
431 dominated by traffic, residential heating (including wood burning), solvent use and natural
432 gas leakage, as was recently shown in Paris (Baudic et al., 2016) but also in other cities
433 (Niedojadlo et al., 2007 in Wuppertal, Germany, Lanz et al., 2008, in Zurich, Switzerland,
434 Morino et al., 2011, in Tokyo, Japan, McCarthy et al., 2013, in Edmonton, CA, USA). VOC
435 levels, diurnal and seasonal variability and source contributions in Paris have been
436 thoroughly described by Baudic et al. (2016). Therefore only minimal information is reported
437 here. Ethane and propane are mainly associated with natural gas leakage sources (and to
438 wood burning to a lesser extent), whereas acetylene, ethylene and propene predominantly
439 come from combustion sources (which include wood burning and vehicle exhausts). Finally
440 pentanes are associated with traffic emissions (vehicle exhaust and /or gasoline

441 evaporation). None of them is a tracer of a specific source and therefore characterisation of
442 sources are usually made by using either a ratio approach, often using CO or acetylene as
443 tracer (see Borbon et al., 2013 and references therein) or an approach based on the
444 determination of sources composition profiles (see Baudic et al., 2016 and references
445 therein). The studied compounds usually show a seasonal cycle with a minimum in
446 spring/summer and maximum in fall/winter. This typical seasonal cycle is due to the
447 combination of several factors: emissions (the wood burning source has a pronounced
448 maximum in winter), photochemistry (OH, which presents higher values in summer, is the
449 main sink of all the studied compounds) and finally dynamics (a shallower boundary layer in
450 winter leads to more accumulation of the pollutants). We note that all compounds selected
451 here have a lifetime (which ranges from a few hours for ethylene to almost 40 days for
452 ethane) shorter than CO.

453

454 Ratios obtained during the Multi-CO₂ campaign are reported along with the results
455 obtained for the MEGAPOLI/CO₂-Megaparis campaign in Table 1. For consistency, we note
456 that the comparison is restricted to the MEGAPOLI/CO₂-Megaparis campaign. Indeed ratios
457 presented in this table have been determined according to the method described previously
458 in Section 3.3.1, which differs from the traditional ratio approach (where the ratio directly
459 represents the slope of the scatter plot between two compounds). Ratios between the
460 campaigns appear to agree within a twofold factor (except for $\Delta n\text{-pentane}/\Delta\text{CO}_2$) but
461 present quite heterogeneous results. The previous section mentions the importance of the
462 seasonal variability for the ratio $\Delta\text{CO}/\Delta\text{CO}_2$, as the Multi-CO₂ campaign occurred in fall,
463 whereas the MEGAPOLI/CO₂-Megaparis campaign occurred in winter, associated with a
464 higher residential heating contribution. If seasonality was the main driver of the ratio $\Delta\text{VOC}/$
465 ΔCO_2 , we would observe higher ratios in winter as well (for compounds largely emitted by
466 residential heating like acetylene and ethylene), which is not the case (ratio $\Delta\text{Acetylene}/$
467 ΔCO_2 is not significantly different between both campaigns and $\Delta\text{Ethylene}/\Delta\text{CO}_2$ is lower
468 during MEGAPOLI/CO₂-Megaparis). Another possible driver of the $\Delta\text{VOC}/\Delta\text{CO}_2$ variability
469 between the two campaigns is the inter-annual variation of VOCs (2010 for MEGAPOLI/CO₂-
470 Megaparis, 2013 for Multi-CO₂). Indeed a recent study has shown significant trends of non-
471 methane hydrocarbons in urban and background areas in France (Waked et al., 2016). These
472 trends (from -3.2% to -9.9 %) have been determined for acetylene and ethylene in Paris and
473 are likely explained by efficient emission control regulation. Nevertheless, these trends
474 would suggest lower ratios in 2013 than in 2010, which was not the case. As the temporal
475 variability does not seem to be the main driver of the $\Delta\text{VOC}/\Delta\text{CO}_2$ difference, and given the
476 complexity of VOC emission profiles, which differ within a same source (e.g., emissions from
477 vehicle exhaust vary as a function of motor temperature and engine type, see Salameh et al.,
478 2014 and references therein), we suggest that this difference arises from the heterogeneity
479 of the VOC sources in the vicinity of the two measurements sites. For instance, remember

480 that one, and only one, of the two sites is located close to an expressway. This would imply a
481 low spatial representativeness of our VOC results obtained in very-low wind conditions.

482

483 **5. Conclusion**

484 We have investigated the possibility to characterise local urban emissions through
485 atmospheric mole fraction measurements collected during low wind speed periods. In the
486 case of Paris, we have shown that this approach significantly reduces the sensitivity of the
487 results to the species background level definition, even in the case of CO₂. Thanks to long-
488 term continuous measurements, we have also shown that the low wind speed conditions in
489 the centre of Paris (especially in Jussieu) sample the hours of the day and the days of the
490 week rather evenly, so that the method characterises an average urban atmosphere.

491 The comparison of ratios obtained for the two measurement campaigns, Multi-CO₂
492 and MEGAPOLI/CO₂-Megaparis, shows differences from -120% to +63% for 9 atmospheric
493 species. Such differences may reveal spatial and seasonal variability in the ratios because the
494 two campaigns took place at different sites, during different years and seasons. However,
495 the evolution of the ratios seems to be mainly influenced by the seasonal changes. This
496 seasonal variability was assessed for the CO to CO₂ ratios for the period from February 2013
497 to June 2014, showing a strong anti-correlation with monthly atmospheric temperature,
498 likely linked to seasonal changes in emissions sources (for example, domestic heating is
499 predominant in winter and non-existent in summer). We provide evidence on the
500 importance of residential heating in the total $\Delta\text{CO}/\Delta\text{CO}_2$ ratio. This ratio is higher than the
501 ones for other sectors, which is in contradiction to current estimates from the Airparif
502 inventory. Due to the heterogeneity of VOC sources, ratios that include VOCs are more
503 difficult to interpret in terms of representativeness in low wind speed conditions.

504 The determination of these average ratios may be useful to assess the estimates
505 provided by emission inventories. Indeed, city-scale emission inventories mainly focus on air
506 quality, and the link with greenhouse gases, especially with CO₂, is not well made. The
507 combination of the well-known total pollutant emissions with the ratios estimated by our
508 experimental approach should allow a better quantification of total CO₂ emissions.

509

510 **Acknowledgements:**

511 We acknowledge IPSL (Institut Pierre Simon Laplace) for funding the Multi-CO₂ project as
512 well as the Ville de Paris for funding the project entitled *Le CO₂ parisien* which allowed us to
513 carry out the measurement campaign. We are very grateful to Pascal Jeseq from LERMA for
514 his technical support in Jussieu and to Christof Janssen for this fruitful collaboration. We
515 thank AIRPARIF and particularly Olivier Perrussel for the latest Aiparif inventory and the
516 productive discussions. We are also very grateful Dominique Baisnee, Nicolas Bonnaire and
517 Roland Sarda-Estève for their technical help during the Multi-CO₂ campaign. We
518 acknowledge François Ravetta for the access to the QUALAIR platform. We thank Julie Helle
519 for her technical help. We thank the ICOS-Ramces team for the calibration of the gas tanks
520 to the WMO NOAA scale as well as François Truong and Cyrille Vuillemin for their precious
521 technical advices. We acknowledge the Megapoli and CO₂-Megaparis projects for providing
522 support to this study. This work was also partly supported by CNRS, CEA and UVSQ.

523

524 **References**

- 525 AIRPARIF, Bilan des émissions de polluants atmosphériques et de gaz à effet de serre en Île-
526 de-France pour l'année 2010 et historique 2000/2005 : Méthodologie et résultats, Juillet
527 2013.
- 528 Ammoura, L., Xueref-Remy, I., Gros, V., Baudic, A., Bonsang, B., Petit, J.-E., Perrussel, O.,
529 Bonnaire, N., Sciare, J., and Chevallier, F.: Atmospheric measurements of ratios between
530 CO₂ and co-emitted species from traffic: a tunnel study in the Paris megacity, *Atmos. Chem.*
531 *Phys.*, 14, 12871-12882, doi:10.5194/acp-14-12871-2014, 2014.
- 532 Bellassen, V. and Stephan, N.: Accounting for Carbon : Monitoring, Reporting and Verifying
533 Emissions in the Climate Economy, Cambridge University Press, Cambridge, UK, 2015.
- 534 BIPM: Vocabulaire international de métrologie - Concepts fondamentaux et généraux et
535 termes associés (VIM, 3^e édition), Tech. Rep. JCGM 200 :2012, available at
536 <http://www.bipm.org/fr/publications/guides/vim.html> (last access: November 2015), 2012.
- 537 Borbon, A., Gilman, J. B., Kuster, W. C., Grand, N., Chevallier, S., Colomb, A., Dolgorouky,
538 C., Gros, V., Lopez, M., Sarda-Esteve, R., Holloway, J., Stutz, J., Petetin, H., McKeen, S.,
539 Beekmann, M., Warneke, C., Parrish, D. D., and de Gouw, J. A.: Emission ratios of
540 anthropogenic volatile organic compounds in northern mid-latitude megacities:
541 Observations versus emission inventories in Los Angeles and Paris, *J. Geophys. Res.*
542 *Atmos.*, 118, 2041–2057, doi:10.1002/jgrd.50059, 2013.
- 543 Bréon, F. M., Broquet, G., Puygrenier, V., Chevallier, F., Xueref-Remy, I., Ramonet, M.,
544 Dieudonné, E., Lopez, M., Schmidt, M., Perrussel, O., and Ciais, P.: An attempt at estimating
545 Paris area CO₂ emissions from atmospheric concentration measurements, *Atmos. Chem.*
546 *Phys.*, 15, 1707-1724, doi:10.5194/acp-15-1707-2015, 2015.
- 547 Brown, S.G., Frankel, A. and Hafner, H.R.: Source apportionment of VOCs in the Los Angeles
548 area using positive matrix factorization, *Atmos. Environ.*, 41, 227-237, doi:
549 10.1016/j.atmosenv.2006.08.021, 2007.
- 550 Chevallier, F., Ciais P., Conway T. J., Aalto T., Anderson B. E., Bousquet P., Brunke E. G.,
551 Ciattaglia L., Esaki Y., Fröhlich M., Gomez A.J., Gomez-Pelaez A.J., Haszpra L., Krummel P.,
552 Langenfelds R., Leuenberger M., Machida T., Maignan F., Matsueda H., Morguá J. A., Mukai
553 H., Nakazawa T., Peylin P., Ramonet M., Rivier L., Sawa Y., Schmidt M., Steele P., Vay S. A.,
554 Vermeulen A. T., Wofsy S., Worthy D.: CO₂ surface fluxes at grid point scale estimated from a
555 global 21-year reanalysis of atmospheric measurements. *J. Geophys. Res.*, 115, D21307,
556 doi:10.1029/2010JD013887, 2010.
- 557 Dolgorouky, C., Gros, V., Sarda-Esteve, R., Sinha, V., Williams, J., Marchand, N., Sauvage, S.,
558 Poulain, L., Sciare, J., and Bonsang, B.: Total OH reactivity measurements in Paris during the

559 2010 MEGAPOLI winter campaign, *Atmos. Chem. Phys.*, 12, 9593–9612, doi:10.5194/acp-12-
560 9593-2012, 2012.

561 EEA 2014: Air quality in Europe – 2014 report, European Environment Agency, available at:
562 <http://www.eea.europa.eu/publications/air-quality-in-europe-2014> (last access: April 2015),
563 doi: 10.2800/22847, 2014.

564 Gros, V., Gaimoz, C., Herrmann, F., Custer, T., Williams, J., Bonsang, B., Sauvage, S., Locoge,
565 N., d'Argouges, O., Sarda-Esteve, R., and Sciare, J.: Volatile Organic Compounds sources in
566 Paris in spring 2007. Part I: Qualitative analysis, *Environ. Chem.*, 8, 74–90,
567 doi:10.1071/en10068, 2011.

568 INSEE, La population légale en Île-de-France au 1er Janvier 2012, *Insee Flash*, n°1, Décembre
569 2014.

570 Lanz, V. A., Hueglin, C., Buchmann, B., Hill, M., Locher, R., Staehelin, J. and Reimann, S.:
571 Receptor modeling of C2 - C7 hydrocarbon sources at an urban background site in Zurich,
572 Switzerland: changes between 1993-1994 and 2005-2006, *Atmos. Chem. Phys.*, 8, 2313-
573 2332, doi:10.5194/acp-8-2313-2008, 2008.

574 Lauvaux T., Miles N. L., Richardson S.J., Deng A., Stauffer D.R., Davis K. J., Jacobson G., Rella
575 C., Calonder G.-P., and DeCola P. L.: Urban Emissions of CO₂ from Davos, Switzerland: The
576 First Real-Time Monitoring System Using an Atmospheric Inversion Technique. *J. Appl.*
577 *Meteor. Climatol.*, 52, 2654–2668, doi: <http://dx.doi.org/10.1175/JAMC-D-13-038.1>, 2013.

578 Levin, I., and Karstens, U.: Inferring high-resolution fossil fuel CO₂ records at continental
579 sites from combined 14CO₂ and CO observations, *Tellus B*, 59(2), 245-250, 2007.

580 Lopez, M., Schmidt, M., Delmotte, M., Colomb, A., Gros, V., Janssen, C., Lehman, S. J.,
581 Mondelain, D., Perrussel, O., Ramonet, M., Xueref-Remy, I., and Bousquet, P.: CO,
582 NO_x and ¹³CO₂ as tracers for fossil fuel CO₂: results from a pilot study in Paris during winter
583 2010, *Atmos. Chem. Phys.*, 13, 7343–7358, doi:10.5194/acp-13-7343-2013, 2013.

584 Miller, J. B., S. J. Lehman, S. A. Montzka, C. Sweeney, B. R. Miller, C. Wolak, E. J.
585 Dlugokencky, J. R. Southon, J. C. Turnbull, and P. P. Tans: Linking emissions of fossil fuel
586 CO₂ and other anthropogenic trace gases using atmospheric ¹⁴CO₂, *J. Geophys. Res.*, 117,
587 D08302, doi:10.1029/2011JD017048, 2012.

588 Morino, Y., Ohara, T., Yokouchi, Y and Ooki, A.: Comprehensive source apportionment of
589 volatile organic compounds using observational data, two receptor models, and an emission
590 inventory in Tokyo metropolitan area, *J. Geophys. Res.*, 116, D0211,
591 doi:10.1029/2010JD014762, 2011.

592 Niedojadlo, A., Heinz Becker, K., Kurtenbach, R. and Wiesen, P.: The contribution of traffic
593 and solvent use to the total NMVOC emission in a German city derived from measurements

594 and CMB modelling, *Atmos. Environ.*, 41, 7108–7126, doi:10.1016/j.atmosenv.2007.04.056,
595 2007.

596 Saide, P., Bocquet, M., Osses, A., and Gallardo, L. : Constraining surface emissions of air
597 pollutants using inverse modelling: method intercomparison and a new two-step two-scale
598 regularization approach, *Tellus B*, 63: 360–370. doi: 10.1111/j.1600-0889.2011.00529.x,
599 2011.

600 Salameh, T., Borbon, A., Afif, C., Sauvage, S., Locoge, N. and Granier, C. : Speciation of
601 anthropogenic VOC emissions from observations in contrasted urban environments: a basis
602 for emission inventory evaluation and the definition of CMIP (Coupled Model
603 Intercomparison Project) historical emission inventory, *Our Common Future under Climate
604 Change*, 1114, 2015.

605 SETRA: Emissions routières de polluants atmosphériques : courbes et facteurs d'influence,
606 available at: [http://catalogue.setra.fr/ documents/Cataloguesetra/0005/Dtrf-
607 0005666/DT5666.pdf](http://catalogue.setra.fr/documents/Cataloguesetra/0005/Dtrf-0005666/DT5666.pdf) (last access: September 2015), 2009.

608 Touaty, M., and Bonsang, B.: Hydrocarbon emissions in a highway tunnel in the Paris area,
609 *Atmos. Environ.*, 34, 985-996, 2000.

610 Turnbull J.C., Sweeney C., Karion A., Newberger T., Lehman S.J., Tans P.P., Davis K.J., Lauvaux
611 T., Miles N.L., Richardson S.J., Cambaliza MO, Shepson P.B., Gurney K., Patarasuk R. and
612 Razlivanov I.: Toward quantification and source sector identification of fossil fuel CO₂
613 emissions from an urban area: Results from the INFLUX experiment, *J. Geophys. Res.*
614 *Atmos.*, 120,292–312, doi:10.1002/2014JD022555, 2015.

615 Turnbull, J. C., Karion, A., Fischer, M. L., Faloona, I., Guilderson, T., Lehman, S. J., Miller, B. R.,
616 Miller, J. B., Montzka, S., Sherwood, T., Saripalli, S., Sweeney, C., and Tans, P. P.: Assessment
617 of fossil fuel carbon dioxide and other anthropogenic trace gas emissions from airborne
618 measurements over Sacramento, California in spring 2009, *Atmos. Chem. Phys.*, 11, 705-721,
619 doi:10.5194/acp-11-705-2011, 2011.

620 Turnbull, J. C., Miller, J. B., Lehman, S. J., Tans, P. P., Sparks, R. J., and Southon, J.:
621 Comparison of 14CO₂, CO and SF₆ as tracers for recently added fossil fuel CO₂ in the
622 atmosphere and implications for biological CO₂ exchange, *Geophys. Res. Lett.*, 33, L01817,
623 doi:10.1029/2005GL024213, 2006.

624 UNEP 2013: The Emissions Gap Report 2013, United Nations Environment Programme
625 (UNEP), Nairobi, available at : <http://www.unep.org/pdf/UNEPemissionsGapReport2013.pdf>
626 (last access: April 2015), 2013.

627 Vogel, F. R., S. Hammer, A. Steinhof, B. Kromer, and I. Levin, Implication of weekly and
628 diurnal ¹⁴C calibration on hourly estimates of CO-based fossil fuel CO₂ at a moderately

629 polluted site in southwestern Germany, *Tellus B*, 62(5), 512–520, doi:10.1111/j.1600-
630 0889.2010.00477.x, 2010.

631 Vogel, F. R., Levin, I., & Worthy, D. E. : Implications for Deriving Regional Fossil Fuel CO₂
632 Estimates from Atmospheric Observations in a Hot Spot of Nuclear Power Plant 14CO₂
633 Emissions. *Radiocarbon*, 55(2–3), 1556-1572, 2013.

634 Waked, A., Sauvage, S., Borbon, A., Gauduin, J., Pallares, C., Vagnot, M.P., Léonardis, T. and
635 Locoge, N. : Multi-year levels and trends of non-methane hydrocarbon concentrations
636 observed in ambient air in France. *Atm. Env.*, 140, 263-275,
637 doi:10.1016/j.atmosenv.2016.06.059, 2016.

638 Xueref-Remy, I., Dieudonné, E., Vuillemin, C., Lopez, M., Lac, C., Schmidt, M., Delmotte, M.,
639 Chevallier, F., Ravetta, F., Perrussel, O., Ciais, P., Bréon, F.-M., Broquet, G., Ramonet, M.,
640 Spain, T. G., and Ampe, C.: Diurnal, synoptic and seasonal variability of atmospheric CO₂ in
641 the Paris megacity area, *Atmos. Chem. Phys. Discuss.*, doi:10.5194/acp-2016-218, in review,
642 2016.

643 Yoshida, H., Mønster, J., and Scheutz, C.: Plant-integrated measurement of greenhouse gas
644 emissions from a municipal wastewater treatment plant, *Water Res.*, 61, 108–118,
645 doi:10.1016/j.watres.2014.05.014, 2014.

646 Yurdakul, S., Civan, M. and Gürdal, T.: Volatile organic compounds in suburban Ankara
647 atmosphere, Turkey: Sources and variability, *Atmospheric Research*, 120-121, 298-311,
648 doi:10.1016/j.atmosres.2012.09.015, 2013.

649 Yver-Kwok, C. E., Müller, D., Caldow, C., Lebègue, B., Mønster, J. G., Rella, C. W., Scheutz, C.,
650 Schmidt, M., Ramonet, M., Warneke, T., Broquet, G., and Ciais, P.: Methane emission
651 estimates using chamber and tracer release experiments for a municipal waste water
652 treatment plant, *Atmos. Meas. Tech. Discuss.*, 8, 2957-2999, doi:10.5194/amtd-8-2957-2015,
653 2015.

654 Zhang X., and Schreifels J.: Continuous emission monitoring systems at power plants in
655 China: Improving SO₂ emission measurement, *Energy Policy*, Volume 39, Issue 11, November
656 2011, Pages 7432-7438, ISSN 0301-4215, doi:10.1016/j.enpol.2011.09.011, 2011.

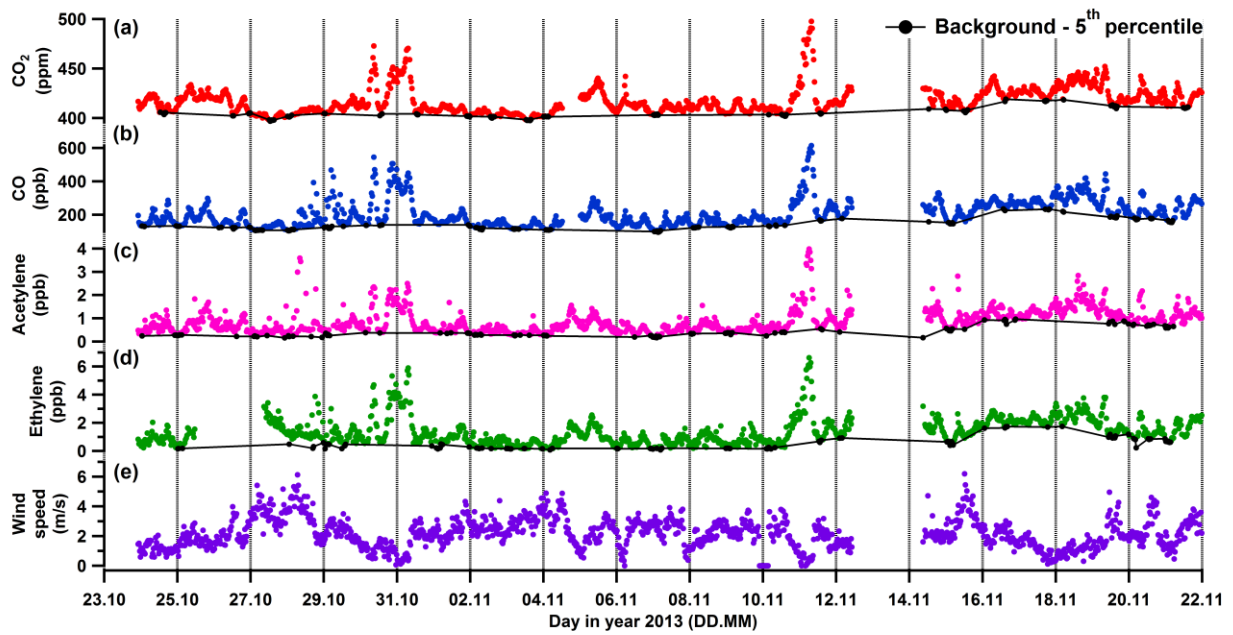
657

658

	ΔCO_2	ΔCO	$\Delta\text{Acetylene}$	$\Delta\text{Ethylene}$	$\Delta\text{Propene}$	$\Delta i\text{-pentane}$	$\Delta n\text{-pentane}$	ΔEthane	$\Delta\text{Propane}$
ΔCO_2	-	5.55/6.33 (0.24)	24.82/25.21 (2.13)	52.55/33.51 (3.87)	11.18/6.26 (2.51)	13.57/11.47 (2.34)	9.27/3.41 (0.97)	49.81/31.70 (5.10)	32.07/20.38 (2.92)
ΔCO		-	3.48/2.78 (0.28)	5.47/5.13 (0.39)	1.32/0.88 (0.08)	2.18/2.04 (0.15)	1.15/0.73 (0.11)	6.56/3.09 (0.59)	3.19/2.27 (0.30)
$\Delta\text{Acetylene}$			-	1.09/0.84 (0.06)	0.21/0.17 (0.01)	0.28/0.34 (0.02)	0.17/0.11 (0.01)	0.75/0.53 (0.10)	0.48/0.35 (0.04)

659

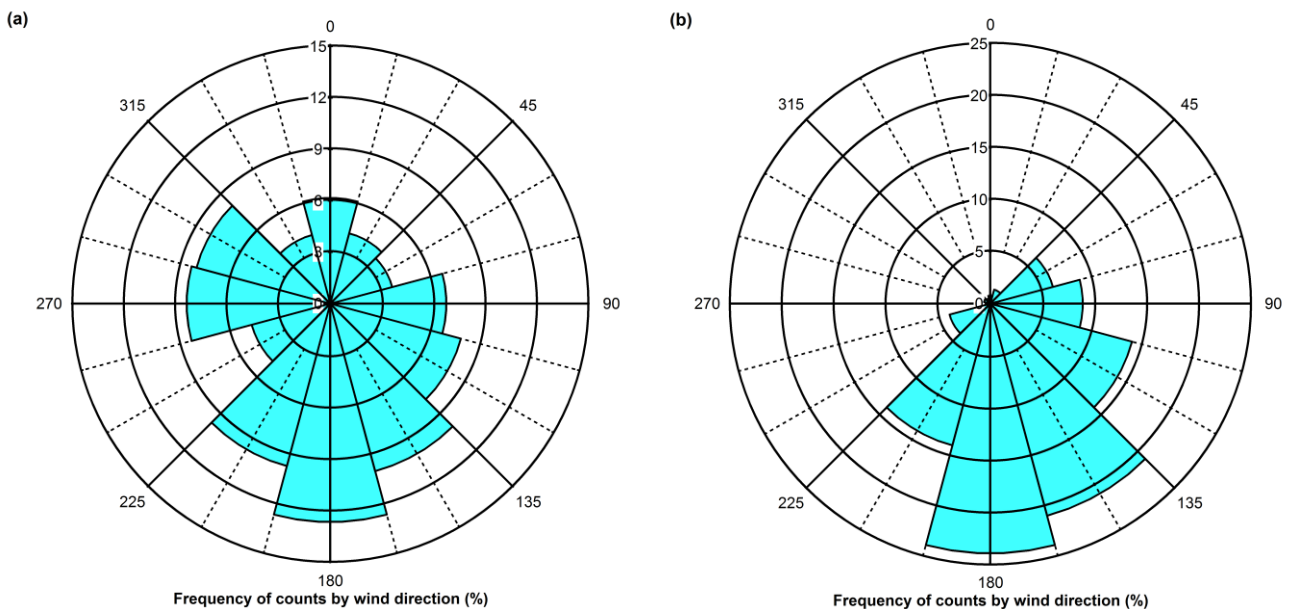
660 **Table 1:** Observed ratios between co-emitted species derived from our method for the Multi-CO₂ and MEGAPOLI/CO₂-Megaparis (in red)
661 campaigns. Numbers in brackets () correspond to 1 σ . The mole fraction ratio is reported in ppb/ppm for $\Delta\text{CO}/\Delta\text{CO}_2$, all others to ΔCO_2 are
662 reported in ppt/ppm. Those that do not include ΔCO_2 are reported in ppb/ppb. Ratios in bold mean that there is a satisfactory agreement
663 between the two campaigns (less than 15% of difference).



664

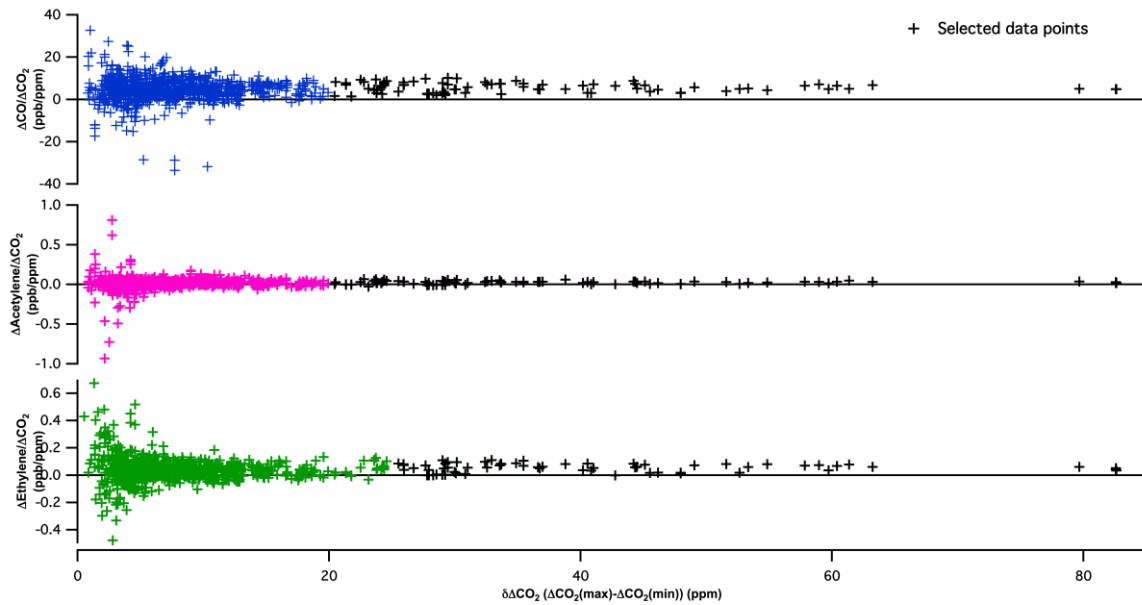
665 **Fig.1: (a-d)** Temporal variation of the mole fraction of selected compounds monitored during
 666 the Multi-CO₂ campaign (30 minutes time step). The black lines represent the background
 667 levels defined with the calculation of the 5th percentile (black disks). **(e)** Wind speed during
 668 the campaign. Time is given in UTC.

669



670

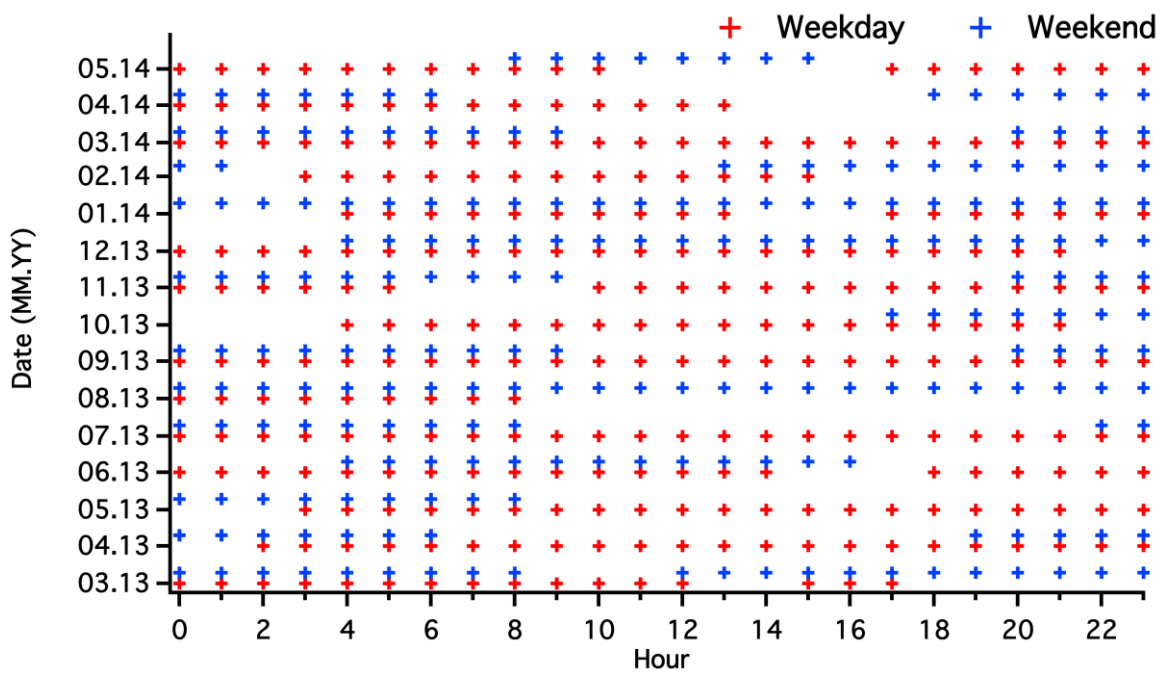
671 **Fig. 2:** Wind roses for two low wind speed situations. **(a)** Wind rose for 10-11 November
 672 2013 (significant peak in mole fractions). **(b)** Wind rose for 18 November 2013 (no significant
 673 peak in mole fractions). The percent scale is not the same for the two wind plots.



674

675 **Fig. 3:** Selected ratios to ΔCO_2 plotted versus the local CO_2 offset ($\delta\Delta\text{CO}_2$) from the
 676 measurements acquired during the Multi- CO_2 campaign. Black data points were selected to
 677 determine the equation of the horizontal asymptote using the criteria described in Section
 678 3.3.2 (the used criteria depend on the considered species).

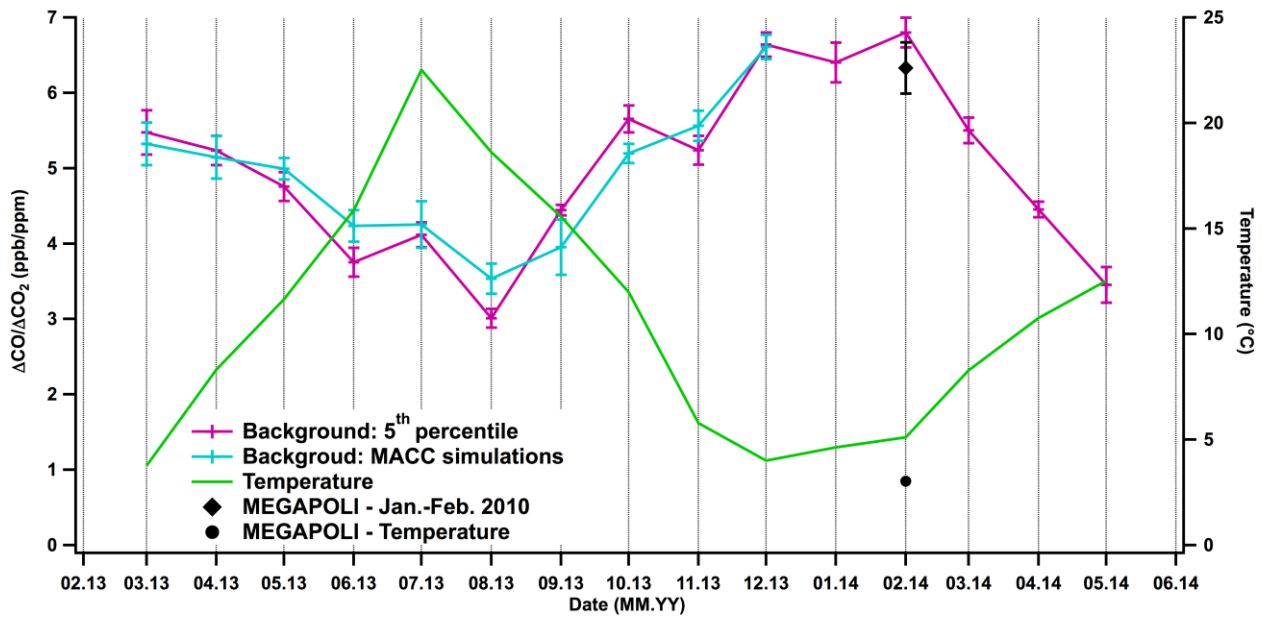
679



680

681 **Fig.4:** Days (weekdays in red crosses and weekends in blue crosses) and hour sampled per
 682 month with our method.

683



684

685 **Fig.5:** Monthly ΔCO to ΔCO_2 ratios in Paris. Results using background levels defined with the
 686 5th percentile are given in violet. The ones using the MACC simulations are in blue. Error bars
 687 on the ratios correspond to 1σ . The ratio from the MEGAPOLI- CO_2 -Megaparis campaign and
 688 the corresponding average temperature are represented by a black disk. Temperature
 689 corresponding to the selected data for the ratio calculation averaged by month is
 690 represented in green as a proxy for season.

691